

IS THE LUNAR MAGNETIC FIELD CORRELATED WITH GRAVITY OR TOPOGRAPHY? S. Gong^{1,2} and M. A. Wieczorek² ¹Key Laboratory of Planetary Sciences, Shanghai Astronomical Observatory, Shanghai 20030, China (sxgong@shao.ac.cn) ²Institut de Physique du Globe de Paris, 75013 Paris, France.

Introduction: Magnetic fields generated by dynamos in the metallic cores of planets are common phenomena in our solar system. Mercury, Earth, and the icy satellite Ganymede have core dynamos that operate today, and magnetic field observations of Mars suggest that it might have once have possessed a dynamo in its past. Somewhat surprisingly, magnetic field measurements made from both the surface and orbit show that portions of the Moon's crust are strongly magnetized [1-3], and paleomagnetic measurements of lunar samples suggest that a dynamo might have lasted for over a billion years [4].

Regardless, the origin of the strong crustal anomalies on the Moon remains enigmatic. The vast majority of lunar magnetic anomalies have no clear correlation with known geologic structures. The sources of lunar magnetic anomalies likely lie below the surface, but it is not known whether these sources are related to basin ejecta, basin impact-melt sheets, ancient lava flows, magmatic intrusions, or magnetized highland materials [5-9].

If there is no clear correlation between the majority of magnetic anomalies and geologic structure, it might be expected that the magnetic field would correlate with gravity given that the primary magnetic carrier in lunar rocks is metallic iron, which is considerably denser than the silicate minerals that make up the crust. If the magnetic anomalies were formed by magmatic intrusions, or basin ejecta, it might be expected that there would also be a correlation between surface topography and magnetic field strength.

Here we test whether such correlations exist by using magnetic field maps derived from the Kaguya and Lunar Prospector missions (as shown in Figure 1) [10], gravity data derived from the Gravity Recovery and Interior Laboratory (GRAIL) mission [11] and topography data derived from the laser altimeter on the Lunar Reconnaissance Orbiter mission [12]. We search for correlations in both the spatial and spectral domains, and quantify the probability that such correlations could have occurred by chance.

Space Correlations: We first search for correlations in the space domain by using a moving window with an angular radius of 6°. By taking all the data within the window, we calculate the correlation between the total magnetic field intensity and either the total gravity anomaly or surface relief. For the gravity field, we consider both the total free-air and Bouguer anomalies. For each location where the analysis is performed on the surface, a single value of the correlation is obtained, which we show in Figure 2.

Considering that the correlation could have occurred by chance, we quantify the probability distribution of the correlation by means of Monte Carlo simulations. Treating the lunar magnetic field as a random stochastic process, 1000 synthetic magnetic fields were generated that satisfied the global power spectrum of the lunar magnetic field. The correlations between total synthetic magnetic field intensity and the other fields were then calculated, from which we computed the probability distribution of the correlation function. We performed Monte Carlo simulations in 7 different regions, and all regions show that 95% of the correlations with either the total gravity anomaly or surface relief are in the range [-0.4, 0.4]. Any observed value greater than 0.4 would hence indicate that the correlation is statistically significant.

As shown in Figure 2, although the correlations between total magnetic field intensity and both gravity and topography are in the range [-0.4, 0.4], there are some regions that possess a relatively high correlation (plotted in black and white), and most of these regions are within or near impact basins. Such examples include Mendel-Rydberg, Crisium, Humboldtianum, Imbrium, and Orientale. In contrast to the magnetic intensity map of Figure 1, there is no obvious nearside-farside asymmetry in the observed correlations.

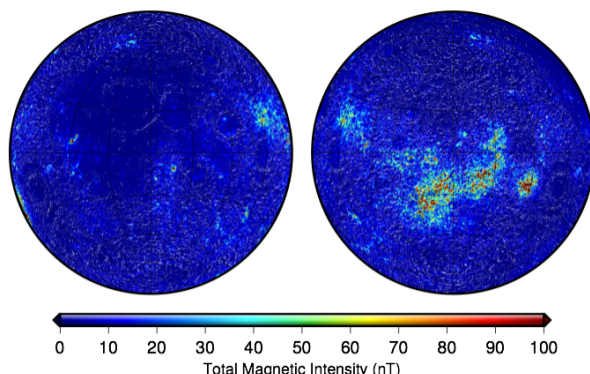


Figure 1. Total intensity of the lunar magnetic field at the surface as derived from Kaguya and Lunar Prospector magnetometer data [10]. Data are presented in two Lambert azimuthal equal-area projections centered over the near- (left) and farside (right) hemispheres. Each image covers 75% of the lunar surface, and grid lines are spaced at 30° intervals.

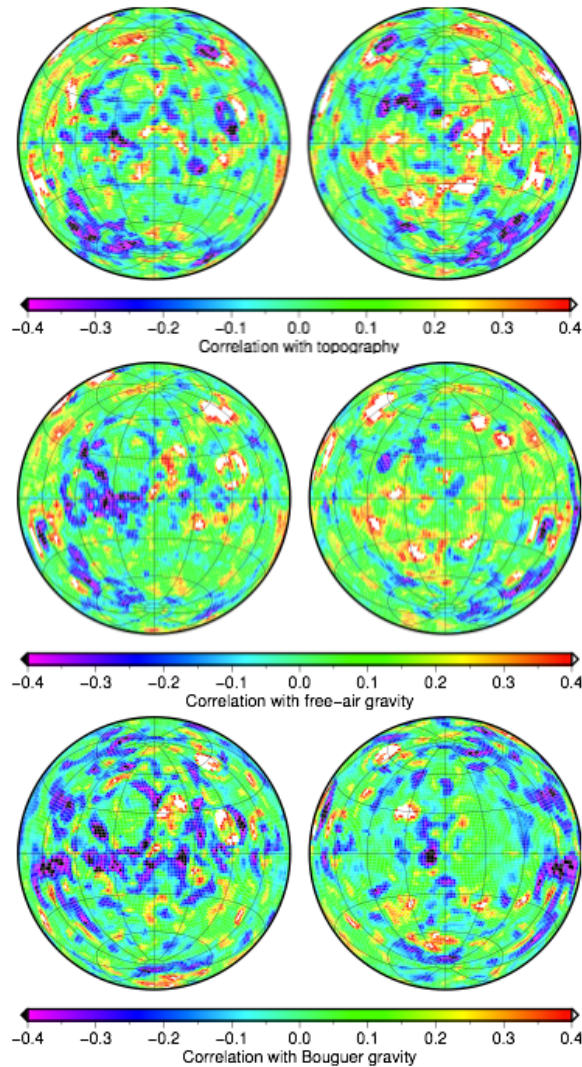


Figure 2. Correlations between total lunar magnetic field intensity and topography (upper), total free-air gravity (middle), and total Bouguer gravity (bottom). The correlation was calculated within circles of angular radius 6° (180 km diameter) at each point on a grid of 60 km spacing. Image format is the same as for Figure 1.

Spectral Correlations: In the previous section, the correlations calculated in the spatial domain provide a single value for each analysis region. Furthermore, this value will be heavily biased by the largest amplitude features in the region. Here, we calculate correlations in the spectral domain using the multitaper spectral analysis approach developed by Wicczorek and Simons [13]. With this technique, a wavelength dependent spectrum of correlations is obtained for each analysis regions.

For our initial attempt, we use windows that are localized within an angular radius of 8° , and which possess a spectral bandwidth of 65 degrees. For these parameters, we have 8 orthogonal windows that possess concentration factors that are greater than 0.99.

As an example, we show the localized correlation spectrum for one point on the lunar farside in Figure 3. Given the 65 degree spectral bandwidth of the window, and the 450 degree bandwidth of the magnetic field, we plot the correlation from spherical harmonic degree 65 to 385. Using a Monte Carlo modelling technique, we also calculated the 1 and 2- σ confidence intervals of the correlation, under the assumption that the magnetic field is a random stochastic process uncorrelated with both gravity and topography. As shown in the figure, the free-air gravity and topography are largely uncorrelated with the magnetic field at the 1- σ confidence limit. Nevertheless, the Bouguer anomaly is found to be correlated at the 95% level with the magnetic potential over a restricted wavelength range between 220 and 350.

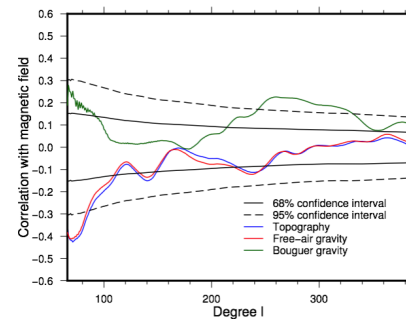


Figure 3. Correlation spectra for a representative region on the farside hemisphere of the Moon ($15^\circ\text{S } 165^\circ\text{W}$). Colored lines show the correlation spectra between the magnetic potential and topography (blue), free-air gravity (red), and Bouguer gravity (green). Data are localized using 8 windows of angular radius 8° (240 km), each with a spherical harmonic bandwidth of 65 degrees. The black solid and dash lines represent respectively the 68% and 95% confidence intervals of the correlations obtained from Monte Carlo simulations.

Conclusion: In order to place constraints on the origin of lunar magnetic anomalies, we have used both space and spectral domain approaches to quantify the correlation between the lunar magnetic field and other geophysical quantities, such as topography, free-air gravity, and Bouguer gravity. Though our results are preliminary, they demonstrate the feasibility of the technique and highlight regions where the correlation is statistically significant. We are currently developing techniques to display the spectral correlation data in map form and to link the regions of high correlation to lunar geologic processes.

References: [1] Dyal P. et al. (1974) *Rev. Geophys. Space Phys.*, 12, 568-591. [2] Hood L. L. et al. (2001) *J. Geophys. Res.*, 106, 27825-27893. [3] Tsunakawa H. et al. (2010) *Space Sci. Rev.*, 154, 219-251. [4] Weiss. B. P. and Tikoo S. M. (2014) *Science* 346(6214), 1246753. [5] Hood L. and Artemieva N. (2008) *Icarus*, 193, 485-502. [6] Wicczorek et al. (2013) *Science* 339, 671-675. [7] Halekas J. et al. (2001) *J. Geophys. Res.*, 106, 27841. [8] Hood L. (2011) *Icarus*, 211, 1109-1128. [9] Purucker et al. (2012) *J. Geophys. Res.*, 117, E05001 [10] Tsunakawa H. et al. (2015) *J. Geophys. Res. Planets*, 120, 1160-1185. [11] Konopliv A. S. et al. (2014) *Geophys. Res. Lett.*, 41, 1452-1458. [12] Smith D. E. et al. (2010) *GRL*, 37(18), L18204. [13] Wicczorek M. A. and Simons F. J. (2007) *J. Fourier Anal. Appl.* 13(6), 665-692.